We are IntechOpen, the world's leading publisher of Open Access books Built by scientists, for scientists

5,300
Open access books available

130,000
International authors and editors

155M
Downloads

Our authors are among the

154
Countries delivered to

TOP 1%
most cited scientists

12.2%
Contributors from top 500 universities

CLARIVATE ANALYTICS
BOOK CITATION INDEX
INDEXED

WEB OF SCIENCE™

Selection of our books indexed in the Book Citation Index
in Web of Science™ Core Collection (BKCI)

Interested in publishing with us?
Contact book.department@intechopen.com

Design and Control of an Omnidirectional Mobile Robot with Steerable Omnidirectional Wheels

Jae-Bok Song*, Kyung-Seok Byun**
*Korea University, ** Mokpo National University
Republic of Korea

1. Introduction

Applications of wheeled mobile robots have recently extended to service robots for the handicapped or the aged and industrial mobile robots working in various environments. The most popular wheeled mobile robots are equipped with two independent driving wheels. Since these robots possess 2 degrees-of-freedom (DOFs), they can rotate about any point, but cannot perform holonomic motion including sideways motion. To overcome this type of motion limitation, omnidirectional mobile robots (OMRs) were proposed. They can move in an arbitrary direction without changing the direction of the wheels, because they can achieve 3 DOF motion on a 2-dimensional plane. Various types of omnidirectional mobile robots have been proposed so far; universal wheels (Blumrich, 1974) (Ilou, 1975), ball wheels (West & Asada, 1997), off-centered wheels (Wada & Mory, 1996) are popular among them.

The omnidirectional mobile robots using omnidirectional wheels composed of passive rollers or balls usually have 3 or 4 wheels. The three-wheeled omnidirectional mobile robots are capable of achieving 3 DOF motions by driving 3 independent actuators (Carlisle, 1983) (Pin & Killough, 1999), but they may have stability problem due to the triangular contact area with the ground, especially when traveling on a ramp with the high center of gravity owing to the payload they carry. It is desirable, therefore, that four-wheeled vehicles be used when stability is of great concern (Muir & Neuman, 1987). However, independent drive of four wheels creates one extra DOF. To cope with such a redundancy problem, the mechanism capable of driving four omnidirectional wheels using three actuators was suggested (Asama et al., 1995).

Another approach to a redundant DOF is to devise some mechanism which uses this redundancy to change wheel arrangements (Wada & Asada, 1999) (Tahboub & Asada, 2000). It is called a variable footprint mechanism (VFM). Since the relationship between the robot velocity and the wheel velocities depends on wheel arrangement, varying wheel arrangement can function as a transmission. Furthermore, it can be considered as a continuously-variable transmission (CVT), because the robot velocity can change continuously by adjustment of wheel arrangements without employing a gear train. The CVT is useful to most mobile robots which have electric motors as actuators and a battery as a power source. Energy efficiency is of great importance in mobile robots because it is directly related to the operating time without

recharging. Some mobile robots are equipped with a transmission system, but most mobile robots use gear trains with a fixed gear ratio, because the transmission is heavy, bulky, and expensive. Therefore, transmission based on wheel arrangement provides possibility of energy efficient drive. The CVT can provide more efficient motor driving capability as its range of velocity ratio gets wider. The mobile robot proposed by (Wada & Asada, 1999), however, has a limited range to ensure stability of the vehicle.

In this research, an omnidirectional mobile robot with steerable omnidirectional wheels (OMR-SOW) shown in Fig. 1 is proposed to improve CVT performance in which robot stability is guaranteed regardless of wheel arrangement and thus the range of velocity ratio is greatly extended. The OMR-SOW is an omnidirectional mobile robot with 3 DOF motion and 1 DOF in steering. The steering DOF can be achieved by synchronously steerable omnidirectional wheels. While the VFM has a common steering axis for all four wheels, the OMR-SOW has an independent steering axis for each wheel. Therefore, the OMR-SOW possesses a wider range of velocity ratio without stability degradation. The four-wheeled omnidirectional mobile robot involving this mechanism combined with the continuous alternate wheels developed in our laboratory (Byun & Song, 2003) has been developed.

Fig. 1. Photo of OMR-SOW.

The OMR-SOW has some drawbacks. When the omnidirectional capability is not required especially, in normal straight-line driving, the omnidirectional mechanism tends to prevent the robot from driving efficiently. In this case, the wheel arrangement used in the automobile (i.e., 4 wheels in parallel) is preferred to the omnidirectional mechanism. Furthermore, the maximum height of a surmountable bump for OMR is limited by the radius of the passive roller of the omnidirectional wheel, which is much smaller than the radius of the wheel for the ordinary mobile robot. To overcome these drawbacks, the robot should function as an ordinary mobile robot unless its task requires omnidirectional capability. In this research, a new mechanism, which can be used as a differential drive mechanism as well as an omnidirectional one, is proposed.

The remainder of this chapter is organized as follows. In Section 2, the structure of a variable wheel arrangement mechanism is introduced and the kinematics and dynamics of the OMR-SOW are presented. Section 3 explains how the CVT function is achieved in the OMR-SOW. Section 4 discusses construction of the OMR-SOW and some experimental results. Conclusions are drawn in Section 5.

2. Omnidirectional Mobile Robot with Steerable Omnidirectional Wheels

In this section, a new type of omnidirectional mobile robot, an omnidirectional mobile robot with steerable omnidirectional wheels (OMR-SOW), is introduced. Since four wheels of a robot can be independently driven, the OMR-SOW is of 4 DOFs: 2 DOFs for translation, 1 DOF rotation and 1 DOF for steering. The steering DOF can function as a continuously variable transmission (CVT). In the following subsections, steerable omnidirectional wheels are introduced and the features of the OMR-SOW are discussed in detail.

2.1 Steerable Omnidirectional Wheels

Nontrivial wheeled mobile robots are classified into five categories according to degree of mobility and degree of steerability (Campion et al., 1996). They did not mention steerable omnidirectional wheels since most omnidirectional wheels did not have steering capability. However, steerable omnidirectional wheels have an additional DOF which can be used as a continuously variable transmission.
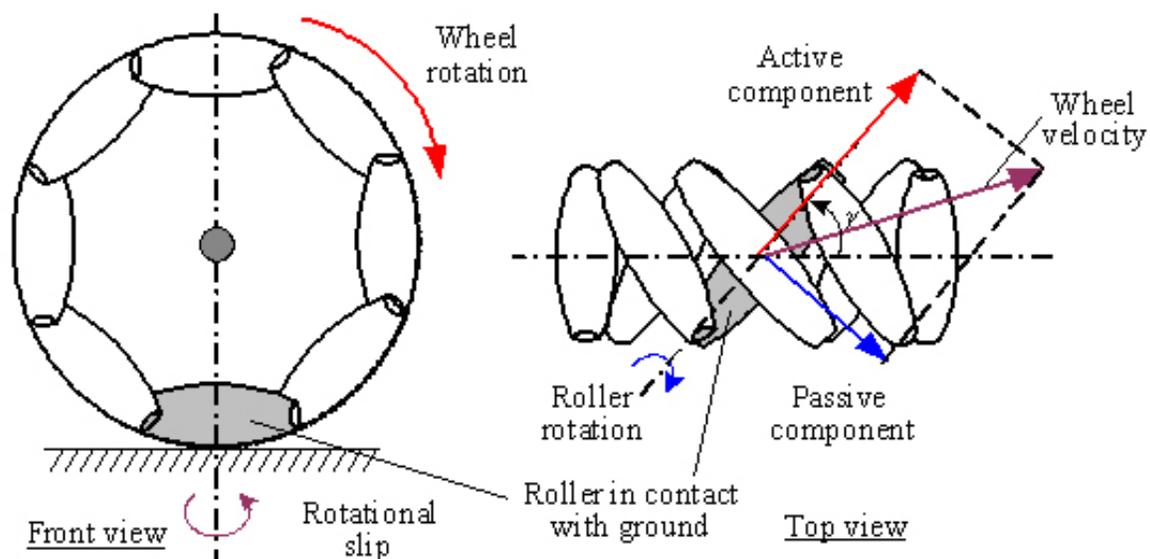

Fig. 2. DOFs in a general omnidirectional wheel.

An omnidirectional wheel has 3 DOFs composed of wheel rotation, roller rotation and rotational slip about the vertical axis passing through the point of contact (Muir & Neuman, 1987). Fig. 2 shows a typical omnidirectional wheel in which the roller axes have an inclination angle γ with the wheel plane. Note that the wheel shown in the figure represents a general omnidirectional wheel and several different wheel mechanisms are available depending on roller types and inclination angles (e.g., universal wheel (Blumrich, 1974) with $\gamma = 0°$ and Mecanum wheel (Ilou, 1975) with $\gamma = 45°$) In the omnidirectional wheel, the wheel velocity can be divided into the components in the active direction and in the passive direction. The active component is directed along the axis of the roller in contact with the ground, while the passive one is perpendicular to the roller axis.

In most cases, omnidirectional wheels are fixed relative to the robot body and do not rotate for steering since steering can be performed by a combination of wheel velocities in these types of mechanisms. Omnidirectional wheels, however, are able to be combined with the steering mechanism as shown in Fig. 3. Since the steering mechanism provides an additional

DOF, this type of steerable omnidirectional wheel module has one more DOF in addition to 3 DOFs defined in Fig. 2. In Fig. 3, the origin o represents the center of a robot and C the steering axis for the wheel shown. In the figure, ϕ is the steering angle, l is the offset distance, L_0 is the distance from the robot center to steering axis, and γ is the angle between the roller axis and the wheel plane, respectively.
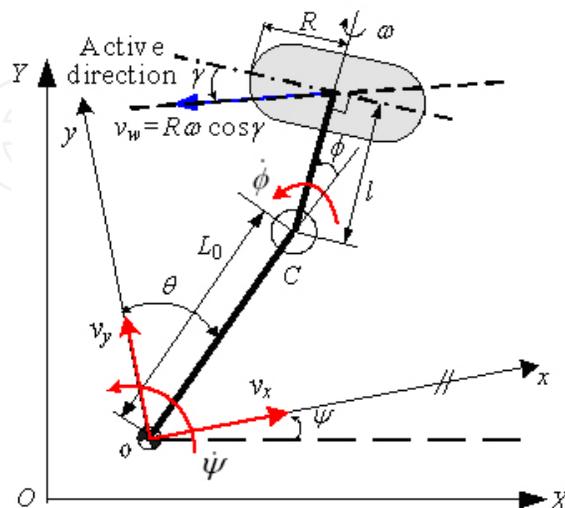

Fig. 3. Coordinate systems and parameters for a steerable omnidirectional wheel.

As mentioned earlier, a steerable omnidirectional wheel has 4 DOFs. Since roller rotation and rotational slip do not impose any constraint on the wheel motion, the constraints can be obtained by the relationship between the robot velocity and the active wheel velocity (i.e., wheel velocity in the active direction). The active wheel velocity is given by

$$v_w = R\omega \cos\gamma \tag{1}$$

where R is the wheel radius and ω is the angular velocity of a wheel.

Let the robot velocity vector be given as $\mathbf{V}_r = [v_x, v_y, \dot{\psi}, \dot{\phi}]^T$, where v_x and v_y are the translational velocities of the robot center, $\dot{\psi}$ is the angular velocity about the robot center, and $\dot{\phi}$ is the derivative of the steering angle, respectively. If the velocity of a robot is given, the velocity of each wheel can obtained as a function of steering angle by

$$\omega = [-v_x \cos(\theta - \phi - \gamma) + v_y \sin(\theta - \phi - \gamma) + \dot{\psi}\{l\cos\gamma + L_0\cos(\gamma + \phi)\} + l\dot{\phi}\cos\gamma]/(R\cos\gamma) \tag{2}$$

The derivation of Eq. (2) can be referred to Song and Byun (2004). Note that a change in steering angle causes the relationship between the robot velocity and the wheel velocities to change, which enables a steerable omnidirectional wheel mechanism to function as a CVT.

Fig. 4 shows the continuous alternate wheel (CAW) (Byun & Song, 2003) which was used in the OMR-SOW. Note that this wheel has the same feature as a general omnidirectional wheel shown in Fig. 2, except for an inclination angle $\gamma = 0^\circ$. Many types of omnidirectional wheels with passive rollers have gaps between rollers. Since these gaps cause a wheel to make discontinuous contact with the ground, they lead to vertical and/or horizontal vibrations during wheel operation. However, the CAW makes continuous contact with the ground with alternating large and small rollers around the wheel, so virtually no vibration is created during operation.
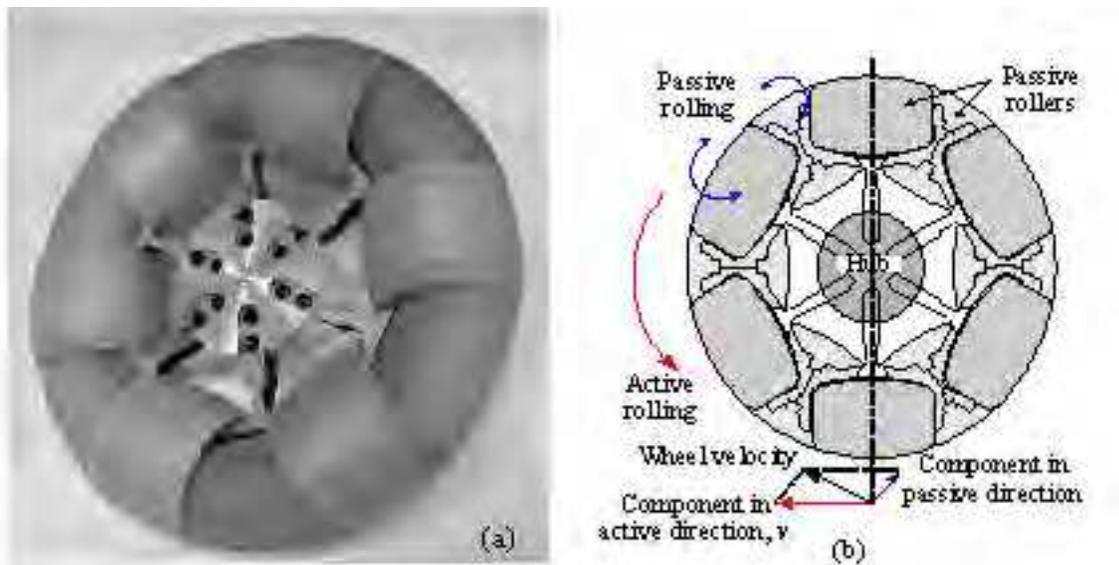
Fig. 4. Continuous alternate wheel; (a) photo and (b) active and passive rolling of CAW.

2.2 OMR-SOW with 4 Offset Steerable Omnidirectional Wheels

In this section, the structure and operational principle of the proposed OMR-SOW will be presented. The coordinate systems for the OMR-SOW are illustrated in Fig. 5. The frame O-XY is assigned as the reference frame for robot motion in the plane, and the moving frame o-xy is attached to the robot center. The angle θ between the y-axis and the diagonal line of the robot body depends on the shape of the body (i.e., $\theta = 45^o$ for a square body). The four wheel modules can rotate about each pivot point C_1, .., C_4 located at the corners of the robot body, but they are constrained to execute a synchronized steering motion of a single DOF by the mechanism composed of connecting links and a linear guide. In Fig. 5, the steering angle ϕ is defined as the angle from the zero position which coincides with the diagonal lines (i.e., C_1C_3 or C_2C_4) of the robot body. Although four wheel modules are steered at each steering axis, the steering angle ϕ for each wheel is identical. Note that steering is indirectly determined by the vector sum of each wheel velocity vector (not by an independent steering motor).
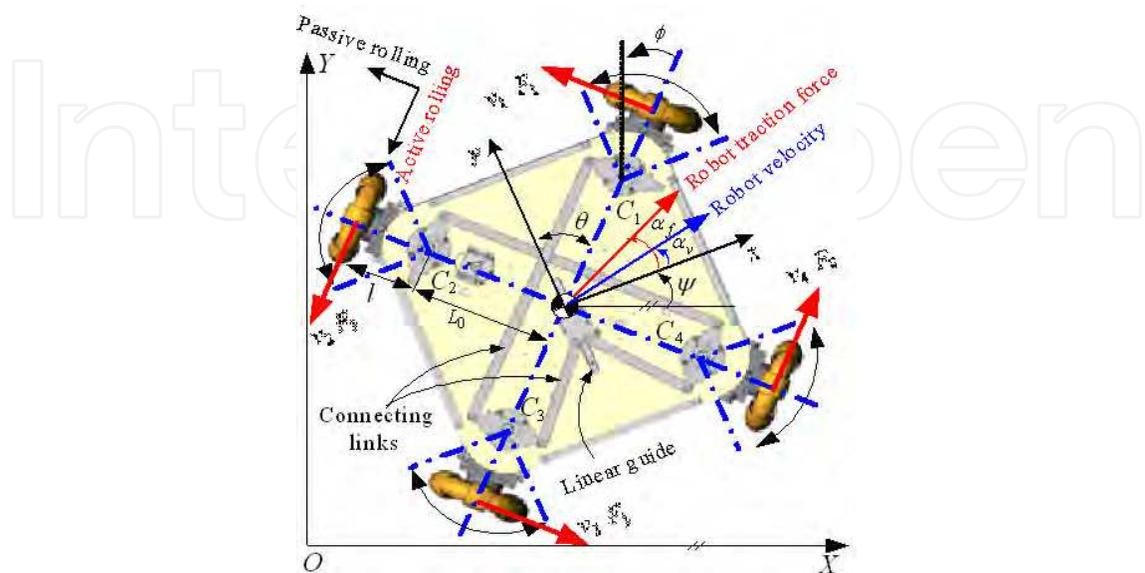

Fig. 5. Coordinate systems for OMR-SOW.

The CAW discussed in section 2.1 can perform differential drive as well as omnidirectional drive. That is, the steering angle is changed in the range of -30º to +30º in the omnidirectional drive mode, but maintained at +45º or -45º in the differential drive mode as shown in Fig. 6. Conventional wheels used in the differential drive have two advantages over omnidirectional wheels. First, the differential drive is generally more efficient in energy than the omnidirectional drive when the omnidirectional drive is not required (e.g., straight-line driving). Second, the conventional wheels can go over a higher bump than the omnidirectional wheels can, because the maximum height of a surmountable bump for the omnidirectional wheels is limited by the radius of its passive roller, which is much smaller than the radius of a conventional wheel.
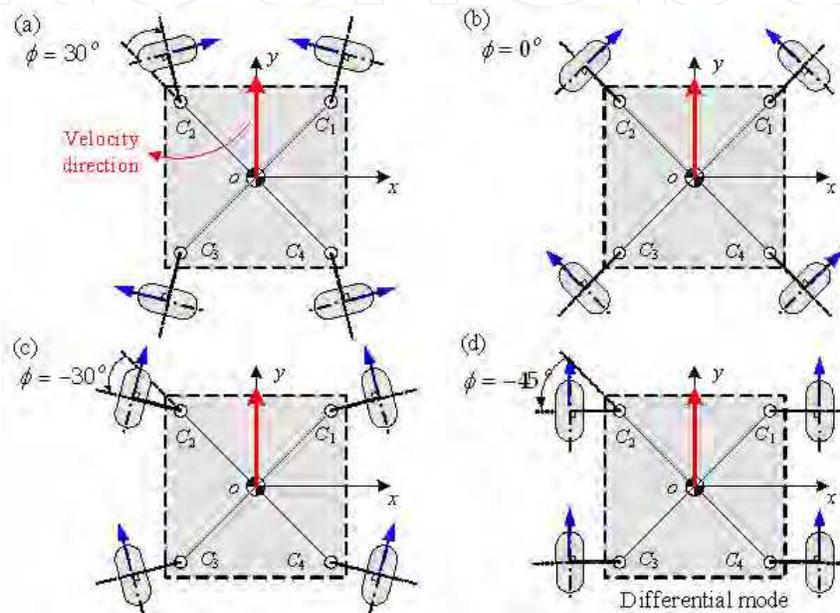

Fig. 6. Various wheel arrangements.

However, the differential drive mode cannot be set up by simply adjusting the steering angle of the omnidirectional wheels to +45° or -45°, because passive rollers cannot be constrained in this case. For example, in Fig. 6(d), pushing the robot in the x direction causes the robot to move in this direction, which does not happen in a robot with conventional wheels which resist sideways motion. That is, passive rolling must not be allowed in the differential drive mode.
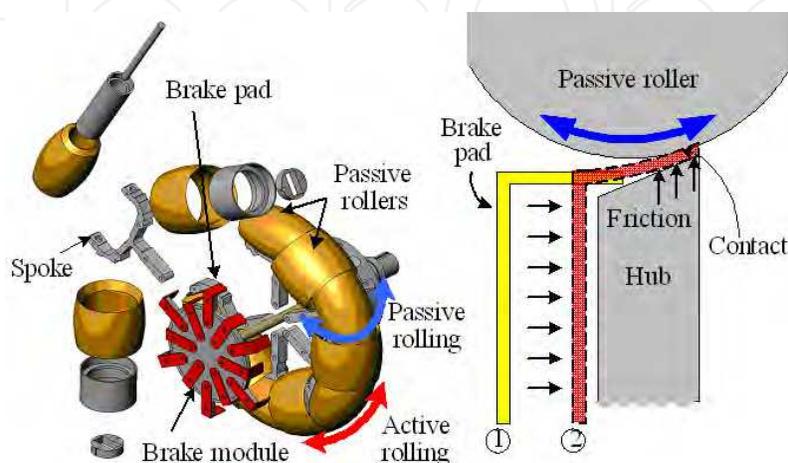

Fig. 7. Disassembled appearance of CAW with brake module.

2.3 Kinematic Analysis of OMR-SOW

The 4-wheeled omnidirectional mobile robot was illustrated in Fig. 5. Using Eq. (2), the relationship between the wheel velocity vector and the vehicle velocity vector can be given by

$$\begin{Bmatrix} v_1 \\ v_2 \\ v_3 \\ v_4 \end{Bmatrix} = \begin{bmatrix} -C & S & L & l \\ -C & -S & L & -l \\ C & -S & L & l \\ C & S & L & -l \end{bmatrix} \begin{Bmatrix} v_x \\ v_y \\ \dot{\psi} \\ \dot{\phi} \end{Bmatrix} \tag{3}$$

where $C = \cos(\theta - \phi)$, $S = \sin(\theta - \phi)$, $L = L_o \cos\phi + l$, and v_1, v_2, v_3, v_4 are the wheel velocities in the active direction. The matrix in Eq. (3) is invertible, since $C \neq 0$ and $S \neq 0$ for $0 < \theta - \phi < 90^o$. The inverse matrix is obtained by

$$\mathbf{J} = \frac{1}{4}\begin{bmatrix} -1/C & -1/C & 1/C & 1/C \\ 1/S & -1/S & -1/S & 1/S \\ 1/L & 1/L & 1/L & 1/L \\ 1/l & -1/l & 1/l & -1/l \end{bmatrix} \tag{4}$$

which corresponds to the Jacobian matrix relating the wheel velocity vector to the robot velocity vector as follows:

$$\mathbf{V}_w = \mathbf{J}^{-1}\mathbf{V}_r \text{ or } \mathbf{V}_r = \mathbf{J}\mathbf{V}_w \tag{5}$$

where $\mathbf{V}_w = [v_1 \ v_2 \ v_3 \ v_4]^T$ and $\mathbf{V}_r = [v_x \ v_y \ \dot{\psi} \ \dot{\phi}]^T$. It follows from Eq. (5) that the robot velocity and steering velocity of the OMR-SOW can be completely determined by control of four independent motors driving each wheel.

To help understanding the operational principle of the OMR-SOW, let us consider the following example. Suppose that the parameters are $\theta = 45^o$, $\phi = -15^o$, $L_O = 2$, $l = 1$, as shown in Fig. 8. If the robot velocity is given by $\mathbf{V}_r = [2 \ 0 \ 0 \ 0]^T$, C, S and L become

$$C = \cos(45^o + 15^o) = 1/2 \quad S = \sin(45^o + 15^o) = \sqrt{3}/2 \quad L = L_o\cos(-15^o) + l = 2.932 \tag{6}$$

Then, Eq. (5) can be calculated as

$$\mathbf{V}_w = \mathbf{J}^{-1}\mathbf{V}_r = \begin{Bmatrix} v_1 \\ v_2 \\ v_3 \\ v_4 \end{Bmatrix} = \begin{bmatrix} -1/2 & \sqrt{3}/2 & 2.932 & 1 \\ -1/2 & -\sqrt{3}/2 & 2.932 & -1 \\ 1/2 & -\sqrt{3}/2 & 2.932 & 1 \\ 1/2 & \sqrt{3}/2 & 2.932 & -1 \end{bmatrix} \begin{Bmatrix} 2 \\ 0 \\ 0 \\ 0 \end{Bmatrix} = \begin{Bmatrix} -1 \\ -1 \\ 1 \\ 1 \end{Bmatrix} \tag{7}$$
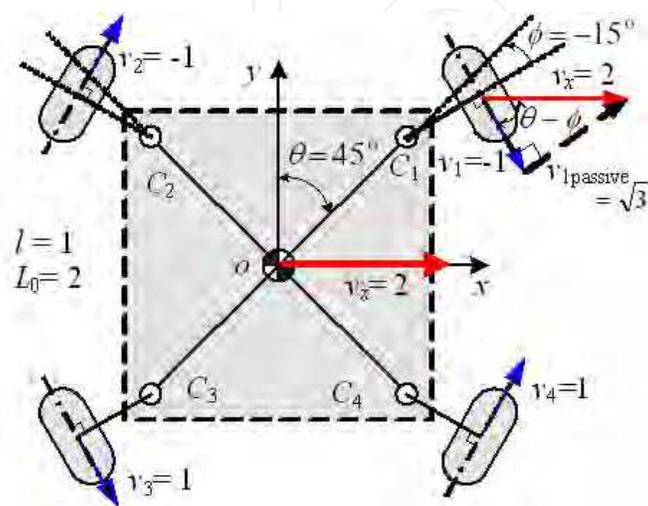

Fig. 8. Example in kinematics.

Fig. 8 shows the active wheel velocities to produce the desired robot velocity. Note that the desired robot velocity contains only the translational velocity in the x direction, so the resultant velocity of each wheel has the magnitude of 2 in the x direction. From this observation, it follows that the passive wheel velocity of wheel 1 has the magnitude of $\sqrt{3}$ to form the specified resultant wheel velocity, as shown in Fig. 8.

2.4 Dynamic Analysis of OMR-SOW

Consider the dynamic model of a robot shown in Fig. 5. The robot motion on the fixed coordinate system XY is described by

$$\mathbf{M}_r \dot{\mathbf{V}}_R = \mathbf{F}_R \tag{8}$$

where $\mathbf{M}_r = \begin{bmatrix} M & 0 & 0 & 0 \\ 0 & M & 0 & 0 \\ 0 & 0 & I_z & 0 \\ 0 & 0 & 0 & I_\phi \end{bmatrix}$, $\mathbf{V}_R = \begin{bmatrix} v_X \\ v_Y \\ \dot{\psi} \\ \dot{\phi} \end{bmatrix}$, and $\mathbf{F}_R = \begin{bmatrix} F_X \\ F_Y \\ T_Z \\ T_\phi \end{bmatrix}$,

where M is the mass of a robot, I_z the moment of inertia about the z axis passing through the robot center and I_ϕ the moment of inertia about the steering axis of the wheel modules. Note that the subscript R represents the fixed reference frame.

The transformation matrix from the moving robot frame $\{r\}$ to the fixed reference frame $\{R\}$ is given by

$$\mathbf{R} = \begin{bmatrix} \cos\psi & -\sin\psi & 0 & 0 \\ \sin\psi & \cos\psi & 0 & 0 \\ 0 & 0 & 1 & 0 \\ 0 & 0 & 0 & 1 \end{bmatrix} \tag{9}$$

The relationship between the fixed reference frame and the moving robot frame is described by

$$\mathbf{V}_R = \mathbf{R} \cdot \mathbf{V}_r \,, \mathbf{F}_R = \mathbf{R} \cdot \mathbf{F}_r \tag{10}$$

Differentiation of V_R is given by

$$\dot{\mathbf{V}}_R = \mathbf{R}\,\dot{\mathbf{V}}_r + \dot{\mathbf{R}}\,\mathbf{V}_r \tag{11}$$

Therefore, the robot of Eq. (8) is described on the moving coordinate system by

$$\mathbf{M}_r(\mathbf{R}\dot{\mathbf{V}}_r + \dot{\mathbf{R}}\mathbf{V}_r) = \mathbf{R}\mathbf{F}_r \text{ or } \mathbf{R}^{-1}\mathbf{M}_r(\mathbf{R}\dot{\mathbf{V}}_r + \dot{\mathbf{R}}\mathbf{V}_r) = \mathbf{F}_r \tag{12}$$

On the other hand, the force and moment of a robot can be expressed from the geometry in Fig. 5 by

$$F_x = -CF_1 - CF_2 + CF_3 + CF_4 \,, \; F_y = SF_1 - SF_2 - SF_3 + SF_4 \tag{13a}$$

$$T_z = LF_1 + LF_2 + LF_3 + LF_4 \,, \; T_\phi = lF_1 - lF_2 + lF_3 - lF_4 \tag{13b}$$

where F_x and F_y are the forces acting on the robot center in the x and y directions, T_z is the moment about the z axis passing through the robot center, and T_ϕ is the torque required to

rotate the wheel modules, respectively. Note that the force F_i ($i = 1, .., 4$) is the traction force acting on the wheel in the direction of active rolling. Using the Jacobian matrix defined in Eq. (4), the relationship between the wheel traction forces and the resultant forces acting on the robot body is given by

$$\mathbf{F}_r = \mathbf{J}^{-T}\mathbf{F}_w \ \text{ or } \ \mathbf{F}_w = \mathbf{J}^T\mathbf{F}_r \tag{14}$$

where $\mathbf{F}_w = [F_1 \ F_2 \ F_3 \ F_4]^T$ and $\mathbf{F}_r = [F_x \ F_y \ T_z \ T_\phi]^T$. It is noted that $\mathbf{F}_r$ is given by a vectorial sum of traction forces. Varying a combination of the traction forces can generate arbitrary forces and moments for driving the vehicle and the moment for steering the wheel modules.

In addition, wheel forces are given by

$$R\,\mathbf{F}_w = \mathbf{U} - I_w\dot{\boldsymbol{\omega}}_w - c_w\boldsymbol{\omega}_w \ \text{ or } \ R\,\mathbf{F}_w = \mathbf{U} - \frac{I_w}{R}\dot{\mathbf{V}}_w - \frac{c_w}{R}\mathbf{V}_w \tag{15}$$

where R is the wheel radius, $\mathbf{U} = [u_1 \ u_2 \ u_3 \ u_4]^T$, where u_i is the motor torque of the i-th motor, I_w is the moment of inertia of the wheel about the drive axis, and c_w is the viscous friction factor of the wheel, and $\boldsymbol{\omega}_w = [\omega_1 \ \omega_2 \ \omega_3 \ \omega_4]^T$, where ω_i is the angular velocity of the i-th wheel. From Eq. (5), the wheel velocity and acceleration vectors are obtained by

$$\mathbf{V}_w = \mathbf{J}^{-1}\mathbf{V}_r \,, \ \ \dot{\mathbf{V}}_w = \dot{\mathbf{J}}^{-1}\mathbf{V}_r + \mathbf{J}^{-1}\dot{\mathbf{V}}_r \tag{16}$$

After substitution of Eq. (14), (15) and (16) into (12), the following relation is obtained

$$\mathbf{R}^{-1}\mathbf{M}_r(\mathbf{R}\dot{\mathbf{V}}_r + \dot{\mathbf{R}}\mathbf{V}_r) = \mathbf{J}^{-T}\mathbf{F}_w = \mathbf{J}^{-T}\left(\frac{1}{R}\mathbf{U} - \frac{I_w}{R^2}(\dot{\mathbf{J}}^{-1}\mathbf{V}_r + \mathbf{J}^{-1}\dot{\mathbf{V}}_r) - \frac{c_w}{R^2}\mathbf{J}^{-1}\mathbf{V}_r\right) \tag{17}$$

This can be simplified by use of the relation $\mathbf{R}^{-1}\mathbf{M}_r\mathbf{R} = \mathbf{M}_r$ to

$$(R\mathbf{J}^T\mathbf{M}_r + \frac{I_w}{R}\mathbf{J}^{-1})\dot{\mathbf{V}}_r + (R\mathbf{J}^T\mathbf{R}^{-1}\mathbf{M}_r\dot{\mathbf{R}} + \frac{I_w}{R}\dot{\mathbf{J}}^{-1} + \frac{c_w}{R}\mathbf{J}^{-1})\mathbf{V}_r = \mathbf{U} \tag{18}$$

Eq. (18) represents the dynamic model of a robot.

3. CVT of OMR-SOW

As explained in Section 2, a change in the steering angle of OMR-SOW functions as a CVT. The CVT of an automobile can keep the engine running within the optimal range with respect to fuel efficiency or performance. Using the engine efficiency data, the CVT controls the engine operating points under various vehicle conditions. A CVT control algorithm for the OMR-SOW ought to include the effects of all four motors. A simple and effective algorithm for control of the CVT is proposed based on the analysis of the operating points of a motor.

3.1 Velocity and Force Ratios

Since the omnidirectional mobile robot has 3 DOFs in the 2-D plane, it is difficult to define the velocity ratio in terms of scalar velocities. Thus the velocity ratio is defined using the concept of norms as follows:

$$r_v = \frac{\|\mathbf{V}_r\|}{\|\mathbf{V}_w\|} = \frac{\|\mathbf{J}\mathbf{V}_w\|}{\|\mathbf{V}_w\|} \tag{19}$$

Note that the velocity ratio for the identical wheel velocities varies depending on the steering angle. For example, suppose that a robot has a translational motion in the x axis. The robot velocity is then given by

$$\mathbf{V}_r = [1 \quad 0 \quad 0 \quad 0]^T \tag{20}$$

From Eq. (4) and (5), the wheel velocity is computed as

$$\mathbf{V}_w = [-C \quad -C \quad C \quad C]^T \tag{21}$$

From Eq. (19), the velocity ratio is obtained as

$$r_v = \frac{1}{2C} = \frac{1}{2\cos(\theta - \phi)} \tag{22}$$

Similarly, if a robot has a translational motion in the y axis, (i.e., $\mathbf{V}_r = [0 \quad 1 \quad 0 \quad 0]^T$), then the velocity ratio is given by

$$r_v = \frac{1}{2S} = \frac{1}{2\sin(\theta - \phi)} \tag{23}$$

For rotational motion given by $\mathbf{V}_r = [0 \quad 0 \quad 1 \quad 0]^T$, the velocity ratio is

$$r_v = \frac{1}{2L} = \frac{1}{2(L_0 \cos\phi + l)} \tag{24}$$

Figure 9 shows the velocity ratio profiles as a function of steering angle in case of L_o = 0.283m, l = 0.19m, and θ = 45 º. It is observed that the translational velocity ratios vary significantly in the range between 0.5 and infinity, while the rotational velocity ratio is kept nearly constant.
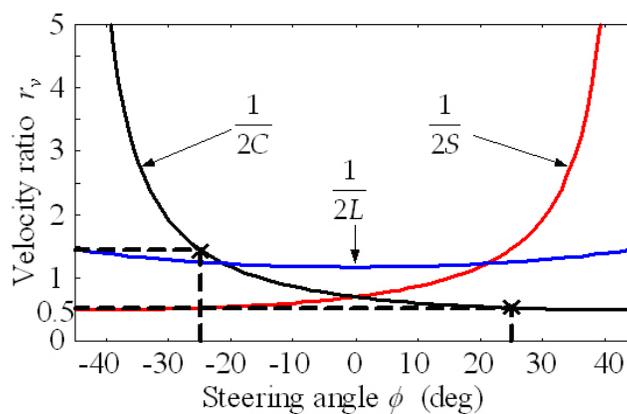

Fig. 9. Velocity ratios as a function of steering angle.

The force ratio of the force acting on the robot center to the wheel traction force can be defined in the same way as the velocity ratio in Eq. (19).

$$r_f = \frac{\|\mathbf{F}_v\|}{\|\mathbf{F}_w\|} = \frac{\|\mathbf{J}^{-T}\mathbf{F}_w\|}{\|\mathbf{F}_w\|} = \frac{1}{r_v} \tag{25}$$

Note that the force ratio corresponds to the inverse of the velocity ratio.

3.2 Motion Control of OMR-SOW

The motion of a mobile robot can be controlled by wheel velocities. From Eq. (5), when the desired robot motion $\mathbf{V}_{rd}$ is given, the reference wheel velocity $\mathbf{V}_{wd}$ of each wheel can be computed by

$$\mathbf{V}_{wd} = \mathbf{J}^{-1} \mathbf{V}_{rd} \tag{26}$$

As shown in Fig. 10 representing the block diagram of the control system for OMR-SOW, when the reference wheel velocity $V_{wd} = [v_{1d}\ v_{2d}\ v_{3d}\ v_{4d}]^T$ is given to each motor, the PI controller performs velocity control of each motor to generate the control signal u_i ($i = 1, .., 4$). If each wheel is controlled to follow the reference wheel velocity, then the robot can achieve the desired motion. Practically, all mobile robots have slip between the wheels and the ground to some extent. This slip causes the real motion to be different from the desired one. Since the robot does not have any sensor measuring the robot velocity, this error is somewhat inevitable.

Since four wheels are independently controlled in the OMR-SOW, a steering angle can be arbitrarily selected while the desired robot velocity (i.e., 2 translational DOF s and 1 rotational DOF) is achieved. That is, a wide range of steering angles can lead to the identical robot velocity. The steering control algorithm then determines the desired steering angle ϕ_d to achieve the maximum energy efficiency for the given robot velocity. Therefore, the desired steering velocity is computed by

$$\dot{\phi}_d = K_\phi(\phi_d - \phi) \tag{27}$$

where K_ϕ is the control gain of steering and ϕ is the actual steering angle measured by the encoder installed on one of the steering axes.
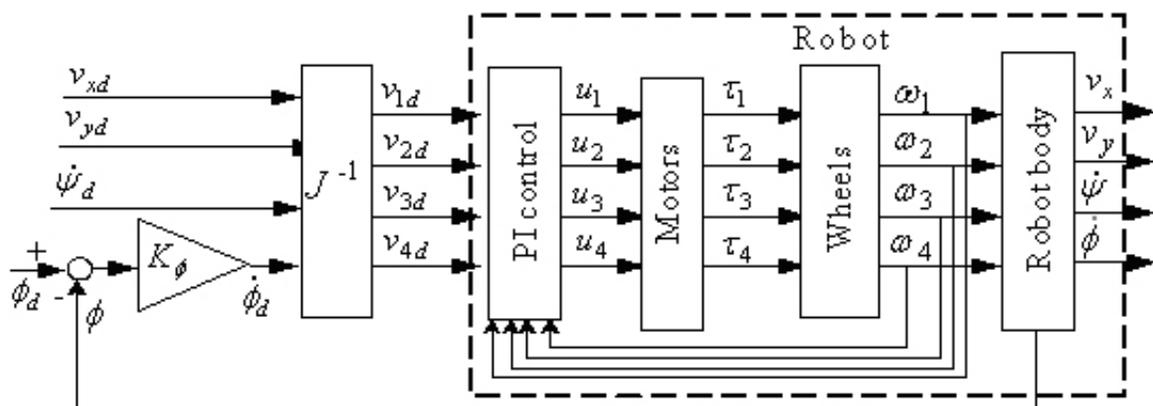

Fig. 10. Control system of OMR-SOW with steering angle control.

Figure 11 shows the operating points of a motor used in the mobile robot. In the figure T_{max} is the maximum continuous torque, and ω_{max} is the maximum permissible angular velocity. The solid lines represent the constant efficiency and the dashed lines denote the constant output power. The input power is obtained by the product of the input current and voltage, whereas the output power is measured by the product of the motor angular velocity and torque. The efficiency η is the ratio of the output to input power.
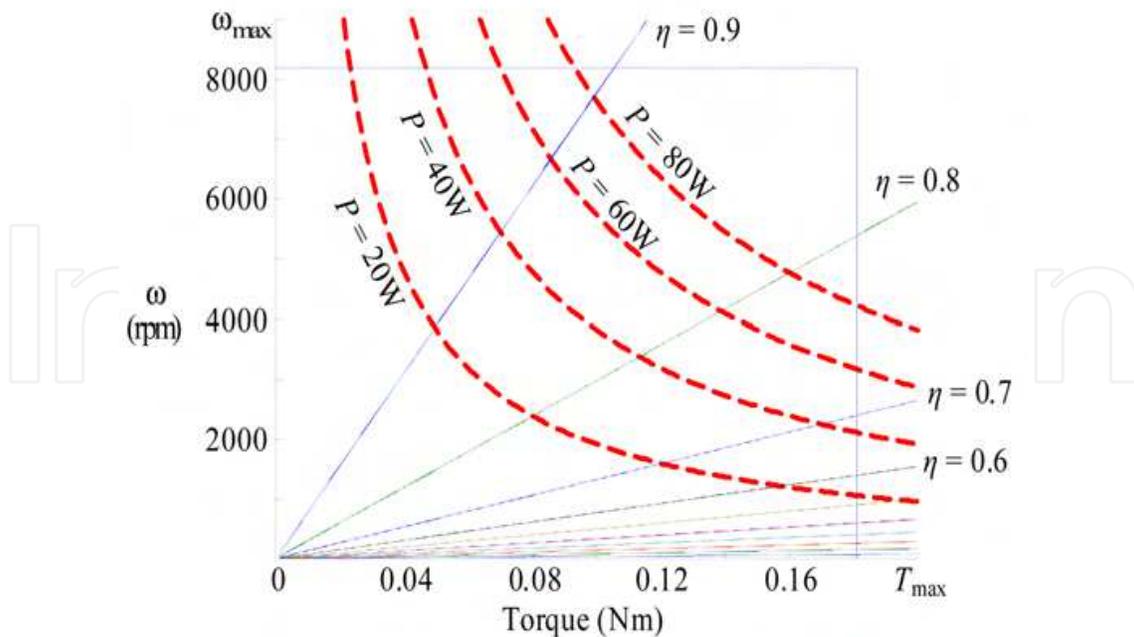
Fig. 11. Operating range of a motor.

As shown in this figure, the efficiency varies as the operating point moves on the constant output power line. The operating point of a motor can be varied by the CVT. For the same output power, a reduction in the force ratio of CVT leads to a decrease in velocity and an increase in torque, and in turn a decrease in efficiency. Therefore, the CVT should be controlled so that motors operate in the region of high velocity and low torque.

3.3 Steering Control Algorithm

As explained in Section 3.2, when the desired robot velocity $\mathbf{V}_{rd}$ is given, each wheel is independently controlled. Any robot velocity can by achieved for a wide range of steering angles, but some steering angles can provide better energy efficiency than others. In this section, the steering control algorithm is proposed to determine such a steering angle that can result in maximum energy efficiency.

In Fig. 11, velocity is controlled by each motor controller. The current sensor at each motor drive measures the motor current and computes the motor torque $\tau = [\tau_1 \ \tau_2 \ \tau_3 \ \tau_4]^T$. The wheel traction force $\mathbf{F}_w$ can then be computed by

$$\mathbf{F}_w = (\tau - I_w \dot{\omega}_w - c_w \omega_w)/r \tag{28}$$

where r is the wheel radius, I_w the moment of inertia of the wheel about the wheel axis, c_w the viscous friction factor of the wheel, and $\omega_w = [\omega_1 \ \omega_2 \ \omega_3 \ \omega_4]^T$ is the wheel angular velocity. By substituting (28) into (14), the robot traction force F_r can be obtained by

$$\mathbf{F}_r = [F_x \ F_y \ T_z \ T_\phi]^T = \mathbf{J}^{-T} \mathbf{F}_w \tag{29}$$

In Eq. (29), the torque T_ϕ required to steer a wheel module is independent of the steering angles. Since the force ratio associated with rotation has little relation with steering angles, it is governed mostly by translational motions. The robot traction force direction α_f can then be given by

$$\alpha_f = \mathrm{atan2}(F_x, F_y) \tag{30}$$

Figure 12 shows the force ratio r_f defined in (25) in terms of the robot traction force angle α_f and the steering angle ϕ. Identical wheel traction forces can generate substantially different robot traction forces depending on ϕ. The OMR-SOW capable of CVT has the maximum energy efficiency in the region with the highest force ratio (i.e., high velocity and low torque). For example, when $\alpha_f = 90^o$, the steering angle of -30° can generate maximum energy efficiency in the omnidirectional drive mode. In Fig. 13, curve 1 is obtained by connecting the steering angles corresponding to the maximum force ratio for each robot traction force angle α_f. However, a rapid change in steering angle from $+30°$ to $-30°$ is required to maintain the maximum force ratio around $\alpha_f = 90^o.n + 45^o$ ($n = 0, 1, …$). Such discontinuity in the steering angle due to a small change in traction force direction is not desirable. To overcome this problem, a sinusoidal profile (curve 2) is practically employed in control of the OMR-SOW.
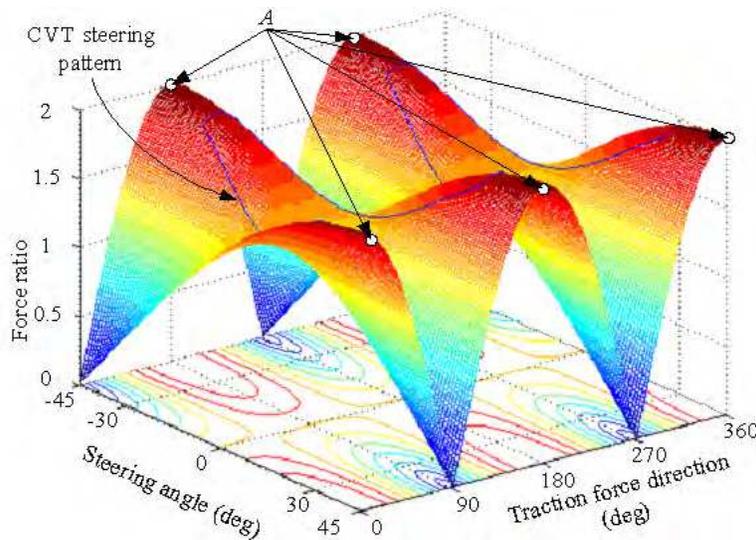

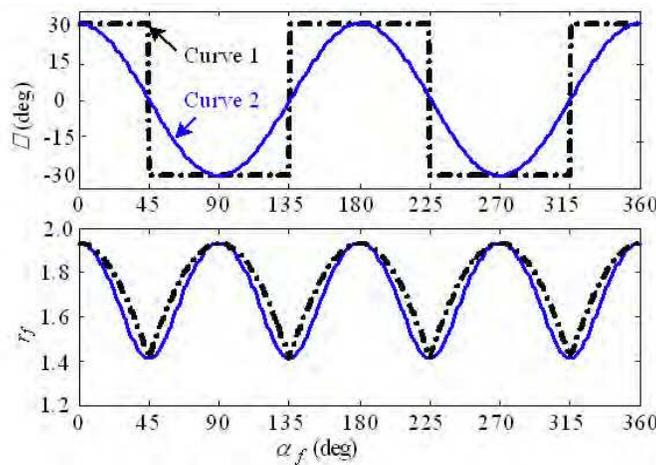Fig. 12. Force ratio as a function of steering angle and force direction.

Fig. 13. Steering angle curve corresponding to maximum force ratio as a function of robot traction force angle.

If the steering angle ϕ is set to either $+45°$ or $-45°$ as shown in Fig. 6(d), the OMR-SOW can be driven in the differential drive mode. In this mode, the OMR-SOW has the maximum force ratio denoted as A as shown in Fig. 12, which leads to the higher energy efficiency

than in the omnidirectional drive mode. In conclusion, if the CVT is controlled in consideration of the steering pattern for each driving condition, the energy efficient driving can be achieved. However, the change from the omnidirectional to the differential drive mode cannot be conducted while the robot is moving, because the steering angle greater than ±30° usually brings about slip between the wheel and ground, and the passive rollers cannot be controlled. Hence, the robot should stop temporarily to conduct this conversion.

4. Experiments and Discussions

4.1 Construction of OMR-SOW

The Omnidirectional Mobile Robot with Steerable Omnidirectional Wheels (OMR-SOW) developed, as shown in Fig. 1. This robot contains four wheel modules comprising the omnidirectional wheel connected to each motor, a synchronous steering mechanism, and a square platform whose side is 500mm. The height of the platform from the ground is 420mm. The robot can be used as a wheelchair since it was designed to carry a payload of more than 100kg. The drive mechanism uses four DC servo motors (150W), which are controlled by the DSP-based motor controllers having a sampling period of 1ms. As shown in Fig. 14, the DSP-based master controller performs kinematic analysis, plans the robot trajectory, and delivers the velocity commands to each wheel. The robot can move autonomously, but the PC is used to monitor the whole system, collect data, and display the robot's states. The suspension system, composed of a 4 bar linkage, a damper and a spring, is required to ensure that all wheels are in contact with the ground at all times, which is very important in this type of four-wheeled mechanism. This suspension can also absorb the shock transmitted to the wheels.
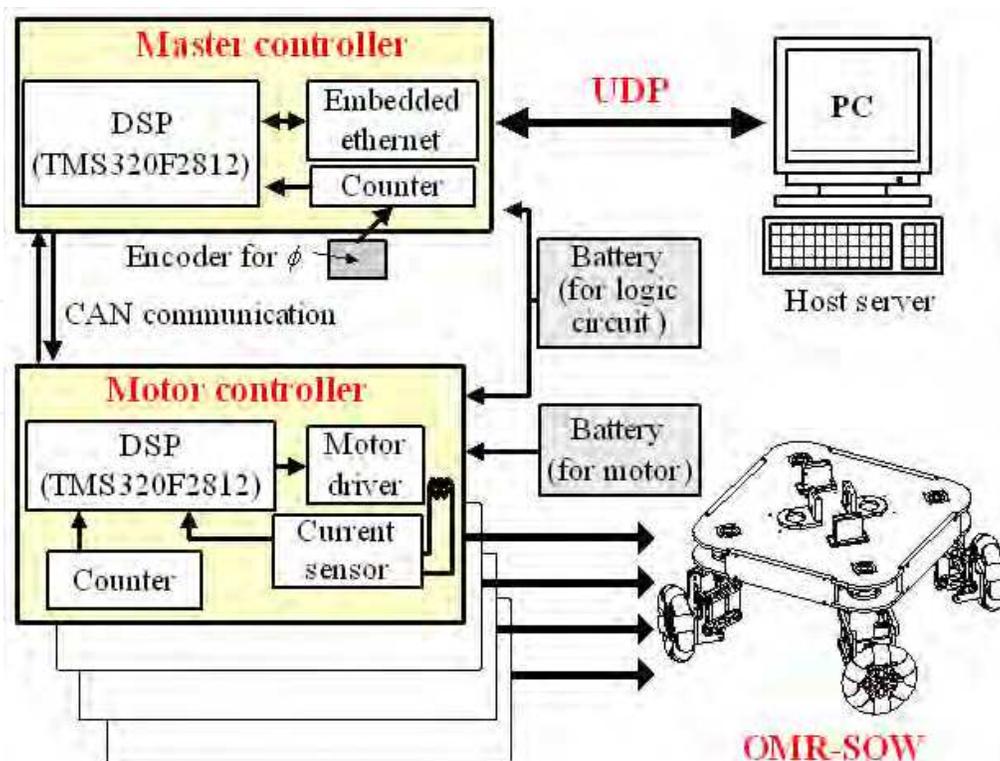

Fig. 14. Control systems for OMR-SOW.

4.2 Experiments of OMR-SOW

Some performance tests for the prototype vehicle have been conducted. Tracking performance of the vehicle with one person on it has been tested for various trajectories. Fig. 15 shows experimental results for a square trajectory. The vehicle control algorithm generates the required vehicle velocity and then computes the velocity of each wheel to achieve the desired motion through the Jacobian analysis given in Eq. (5). In Fig. 15(a), the solid line represents the actual trajectory of the robot and the dashed line is the reference trajectory. Triangles in the figure represent the position and orientation of the robot in every second and the triangle filled with gray color is the start location. Fig. 15(b) shows robot velocity and steering angle. The robot velocity follows the reference input faithfully. Since the accumulated position error is not compensated for, however, there exists a position error between the reference and actual trajectory. Fig. 15(c) shows each wheel velocity and motor currents.
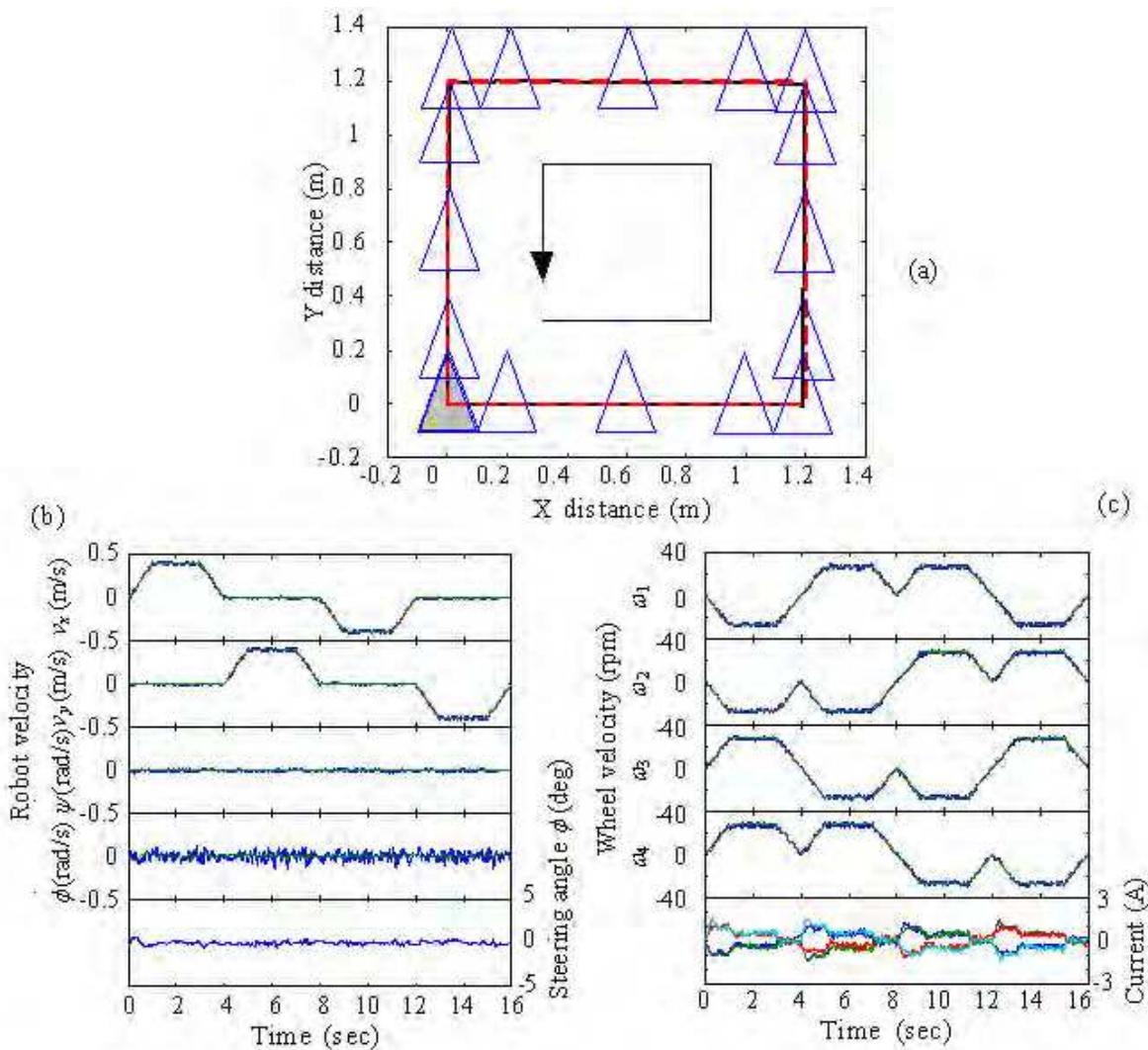

Fig. 15. Experimental results of tracking performance for a rectangular trajectory.

Experiments of Fig. 15 are associated with only translational motions. However, Fig. 16 showing tracking performance for a circular trajectory is associated with both translational and rotational motion. In the experiment, the robot moves in the *x*-direction and simultaneously rotates about the *z*-axis. It is seen that the actual trajectory represented in the

solid line tracks the reference reasonably relatively well. Some error is observed around the finish since the prototype vehicle does not implement any position control algorithm for this test and thus the position error has been accumulated during motion.
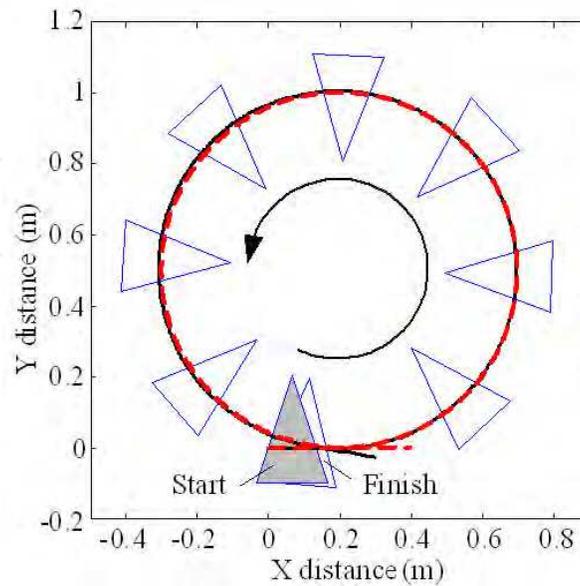

Fig. 16. Experimental results of tracking performance for a circular trajectory.

In the next experiment, a half of the square trajectory existed on a ramp whose slope was 10° as shown in Fig. 17. To follow a given velocity command, the motors should generate much more torque in the ramp than in the ground, so the current is increased. Therefore, the measured current indirectly gives information on the ground conditions or disturbances. Even for a ramp or disturbance, the steering control algorithm based on the measured current can select proper steering angles. The consumed energy was measured as 767.5J for the fixed angle and 653.4J for the case of the steering algorithm, thus showing 14% reduction in energy.
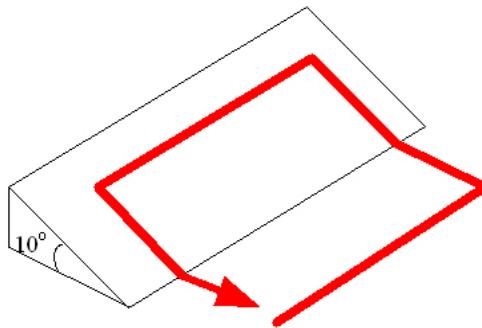

Fig. 17. Square trajectory with ramp.

Next, energy consumption according to the wheel arrangement was investigated. The robot traveled at a speed of 0.05m/s in the *y*-axis in Fig. 6. This motion could be achieved in various wheel arrangements. Among them, 4 configurations were chosen including 3 omnidirectional drive modes and 1 differential drive mode (see Fig. 6). The experimental results are summarized in Table 1. As expected, the differential drive provided better energy efficiency than the omnidirectional drives. This result justifies the proposed mechanism capable of conversion between the omnidirectional and the differential drive mode depending on the drive conditions.

Experiments	ϕ	Average current (A)	Power (W)	Energy (J)
(a)	30	0.385	9.246	924.6
(b)	0	0.296	7.112	711.2
(c)	-30	0.275	6.605	660.5
(d)	-45	0.266	6.402	640.3

Table 1. Comparison of omnidirectional drive with differential drive.

Conventional wheels used in automobiles usually show better performance than the omnidirectional wheels with passive rollers. This is because the height of a surmountable bump for the omnidirectional wheels is limited by the radius of the smallest passive roller and the friction force of the roller. Thus if the passive rollers are constrained not to rotate as in the differential drive mode, even omnidirectional wheels can function as conventional ones. The omnidirectional wheel can go over a 5cm high bump, which is greater than the radius of the passive roller.

5. Conclusions

In this chapter, an omnidirectional mobile robot with steerable omnidirectional wheels (OMR-SOW) has been proposed and the kinematic and dynamic analysis of a proposed robot has been conducted. The motion control system of a robot was developed and various experiments were conducted. As a result of this research, the following conclusions are drawn.
1. The OMR-SOW has 4 DOFs which consist of 3 DOFs for omnidirectional motion and 1 DOF for steering. This steering DOF functions as a continuously variable transmission (CVT). Therefore, the OMR-SOW can be also considered as an omnidirectional mobile robot with CVT.
2. The proposed steering control algorithm for CVT can provide a significant reduction in driving energy than the algorithm using a fixed steering angle. Therefore, the size of an actuator to meet the specified performance can be reduced or the performance such as gradability of the mobile robot can be enhanced for given actuators.
3. Energy efficiency can be further improved by selecting the differential drive mode through the adjustment of OMR-SOW wheel arrangement. The surmountable bump in the differential drive mode is much higher than that in the omnidirectional drive mode.

One of the most important features of the OMR-SOW is the CVT function which can provide energy efficient drive of a robot. If the CVT is not properly controlled, however, energy efficiency capability can be deteriorated. Hence, research on the proper control algorithm is under way for energy efficient drive.

6. References

Asama, H.; Sato, M., Bogoni, L., Kaetsu, H., Masumoto, A. & Endo, I. (1995). Development of an Omnidirectional Mobile Robot with 3 DOF Decoupling Drive Mechanism, *Proc. of IEEE Int. Conf. on Robotics and Automation*, pp. 1925-1930.
Blumrich, J. F. (1974). Omnidirectional vehicle, United States Patent 3,789,947.
Byun, K.-S. & Song, J.-B. (2003). Design and Construction of Continuous Alternate Wheels for an Omni-Directional Mobile Robot, *Journal of Robotic Systems*, Vol. 20, No. 9, pp. 569-579.

Carlisle, B. (1983). An Omnidirectional Mobile Robot, *Development in Robotics*, Kempston, pp. 79-87.

Campion, G.; Bastin, G. & D'Andrea-Novel, B. (1996). Structural Properties and Classification of Kinematic and Dynamic Models of Wheeled Mobile Robot, *IEEE Transactions on Robotics and Automation*, Vol. 12, No. 1, pp. 47-62.

Ilou, B. E. (1975). Wheels for a course stable self-propelling vehicle movable in any desired direction on the ground or some other base, United States Patent 3,876,255.

Muir, P. & Neuman, C. (1987). Kinematic Modeling of Wheeled Mobile Robots, *Journal of Robotic Systems*, Vol. 4, No. 2, pp. 281-340.

Pin, F. & Killough, S. (1999). A New Family of Omnidirectional and Holonomic Wheeled Platforms for Mobile Robot, *IEEE Transactions on Robotics and Automation*, Vol. 15, No. 6, pp. 978-989.

Song. J.-B. & Byun, K.-S. (2004) Design and Control of a Four-Wheeled Omnidirectional Mobile Robot with Steerable Omnidirectional Wheels, *Journal of Robotic Systems*, Vol. 21, No. 4, pp. 193-208

Tahboub, K. & Asada, H. (2000). Dynamic Analysis and Control of a Holonomic Vehicle with Continuously Variable Transmission, *Proc. of IEEE Int. Conf. on Robotics and Automation*, pp. 2466-2472.

Wada, M. & Mory, S. (1996). Holonomic and omnidirectional vehicle with conventional tires, *Proc. of IEEE Int. Conf. on Robotics and Automation*, pp. 3671-3676.

Wada, M. & Asada, H. (1999). Design and Control of a Variable Footprint Mechanism for Holonomic Omnidirectional Vehicles and Its Application to Wheelchairs, *IEEE Trans. on Robotics and Automation*, Vol. 15, No. 6, pp. 978-989.

West, M. & Asada, H. (1997). Design of ball wheel mechanisms for omnidirectional vehicles with full mobility and invariant kinematics, *Journal of Mechanical Design*, pp. 119-161.

Mobile Robotics, Moving Intelligence

Edited by Jonas Buchli

This book covers many aspects of the exciting research in mobile robotics. It deals with different aspects of the control problem, especially also under uncertainty and faults. Mechanical design issues are discussed along with new sensor and actuator concepts. Games like soccer are a good example which comprise many of the aforementioned challenges in a single comprehensive and in the same time entertaining framework. Thus, the book comprises contributions dealing with aspects of the Robotcup competition. The reader will get a feel how the problems cover virtually all engineering disciplines ranging from theoretical research to very application specific work. In addition interesting problems for physics and mathematics arises out of such research. We hope this book will be an inspiring source of knowledge and ideas, stimulating further research in this exciting field. The promises and possible benefits of such efforts are manifold, they range from new transportation systems, intelligent cars to flexible assistants in factories and construction sites, over service robot which assist and support us in daily live, all the way to the possibility for efficient help for impaired and advances in prosthetics.

How to reference

In order to correctly reference this scholarly work, feel free to copy and paste the following:

Jae-Bok Song and Kyung-Seok Byun (2006). Design and Control of an Omnidirectional Mobile Robot with Steerable Omnidirectional Wheels, Mobile Robotics, Moving Intelligence, Jonas Buchli (Ed.), ISBN: 3-86611-284-X, InTech, Available from:
http://www.intechopen.com/books/mobile_robotics_moving_intelligence/design_and_control_of_an_omnidirectional_mobile_robot_with_steerable_omnidirectional_wheels

INTECH
open science | open minds